



## Mixing in the $B_s^0 - \bar{B}_s^0$ System Using Semileptonic Decay Modes And Opposite-Side Flavor Tagging

The DØ Collaboration  
(Dated: March 28, 2005)

$B_s^0 - \bar{B}_s^0$  oscillations were searched for in a large semileptonic sample corresponding to approximately  $460 \text{ pb}^{-1}$  of integrated luminosity accumulated with the DØ Detector in Run II at Fermilab (Tevatron). The flavor of the final state of the  $B_s^0$  meson was determined using the muon charge from the partially reconstructed decay  $B_s^0 \rightarrow \mu^+ D_s^- X$ ,  $D_s^- \rightarrow \phi \pi^-$ ,  $\phi \rightarrow K^+ K^-$ . The opposite-side muon tagging method was used for the initial-state flavor determination. A 95% confidence level limit on the oscillation frequency  $\Delta m_s > 5.0 \text{ ps}^{-1}$  was obtained.

*Preliminary Results for Winter 2005 Conferences*

## I. INTRODUCTION

One of the most interesting topics in  $B$  physics is  $B_s^0$  mixing and measurement of  $\Delta m_s$ . Combining  $\Delta m_s$  and  $\Delta m_d$  would allow to reduce the theoretical uncertainty on  $V_{td}$ . Currently the Tevatron is the only place in the world where  $B_s^0$  mixing can be measured. No measurement of  $B_s^0$  mixing exists, and the current limit is  $\Delta m_s > 14.9 \text{ ps}^{-1}$  at the 95% CL [1]. Global fits to the unitarity triangle give  $\Delta m_s = 18.3 \pm 1.7 \text{ ps}^{-1}$  which is in the range (15.6 – 22.2)  $\text{ps}^{-1}$  at the 95% CL if the current experimental limits on  $\Delta m_s$  are taken into account. Otherwise, global fits give  $\Delta m_s = 20.6 \pm 3.5 \text{ ps}^{-1}$  which is in the range (14.2 – 28.1)  $\text{ps}^{-1}$  at the 95% CL [1].

## II. DETECTOR DESCRIPTION

The following main elements of the DØ detector are essential for this analysis:

- A magnetic central-tracking system, which consists of a silicon microstrip tracker (SMT) and a central fiber tracker (CFT), both located within a 2 T superconducting solenoidal magnet;
- A muon system located beyond the calorimetry.

The SMT has  $\approx 800,000$  individual strips, with typical pitch of 50 – 80  $\mu\text{m}$ , and a design optimized for tracking and vertexing capability at  $|\eta| < 3$ , where  $\eta = -\ln(\tan(\theta/2))$ . The system has a six-barrel longitudinal structure, each with a set of four layers arranged axially around the beam pipe, and 16 radial disks. The CFT has eight thin coaxial barrels, each supporting two doublets of overlapping scintillating fibers of 0.835 mm diameter, one doublet being parallel to the collision axis, and the other alternating by  $\pm 3^\circ$  relative to the axis. Light signals are transferred via clear light fibers to solid-state photon counters (VLPC) that have  $\approx 80\%$  quantum efficiency.

The muon system consists of a layer of tracking detectors and scintillation trigger counters before 1.8 T toroids, followed by two additional layers after the toroids. Tracking at  $|\eta| < 1$  relies on 10 cm wide drift tubes, while 1 cm mini-drift tubes are used at  $1 < |\eta| < 2$ .

## III. DATA SAMPLE

This analysis uses a  $B \rightarrow \mu^+ D_s^- X$  data sample selected with an offline filter from all data taken before September 2004 with no trigger requirement.

The selections for the offline filter are described below.

For this analysis muons were required to have a reconstructed track segment in at least one chamber outside the toroid, to have an associated track in the central tracking system with hits in both SMT and CFT present and to have transverse momentum  $p_T^\mu > 1.5 \text{ GeV}/c$ , pseudo-rapidity  $|\eta^\mu| < 2$  and total momentum  $p^\mu > 3 \text{ GeV}/c$ .

All charged particles in the event were clustered into jets using the DURHAM clustering algorithm [2] with a  $P_t$  cut-off parameter set at 15  $\text{GeV}/c$  [3].

The  $D_s^-$  candidate was constructed from 3 particles included in the same jet as the reconstructed muon. Two of them should give the  $\phi$  meson mass after assigning them kaon masses:  $1.006 < M_{KK} < 1.030 \text{ GeV}$ . The third one should have a charge opposite to the muon charge. All three particles should have hits in the SMT and CFT, transverse momentum  $p_T > 0.7 \text{ GeV}/c$  and pseudo-rapidity  $|\eta| < 2$ . They should form a common  $D_s$ -vertex with  $\chi_D^2 < 16$  of the vertex fit. The vertexing algorithm is described in detail in [4]. For each particle, the axial  $\epsilon_T$  and stereo  $\epsilon_L$  projections of the track impact parameter with respect to the primary vertex together with the corresponding errors ( $\sigma(\epsilon_T)$ ,  $\sigma(\epsilon_L)$ ) were computed. The combined significance  $(\epsilon_T/\sigma(\epsilon_T))^2 + (\epsilon_L/\sigma(\epsilon_L))^2$  was required to be greater than 2 for the pion and at least one of the kaons should have a significance greater than 4. The distance  $d_T^D$  between the primary and  $D$  vertices in the axial plane was required to exceed 4 standard deviations:  $d_T^D/\sigma(d_T^D) > 4$ . The angle  $\alpha_T^D$  between the  $D_s^-$  momentum and the direction from the primary to  $D_s^-$  vertex in the axial plane should satisfy the condition:  $\cos(\alpha_T^D) > 0.9$ .

The tracks of the muon and  $D_s^-$  candidate should produce a common  $B$ -vertex with  $\chi_B^2 < 9$  of vertex fit. The transverse momentum of a  $B_s^0$ -hadron  $P_T^{\mu D_s^-}$  was defined as the vector sum of transverse momenta of muon and  $D_s^-$ . The mass of the  $(\mu^+ D_s^-)$  system should be within the limits:  $1.5 < M(\mu^+ D_s^-) < 5.5 \text{ GeV}/c^2$ . The transverse decay length of a  $B_s^0$ -hadron  $d_T^B$  was defined as the distance in the axial plane between the primary vertex and the vertex produced by the muon and  $D_s^-$ . The distance  $d_T^B$  was allowed to be greater than  $d_T^D$ , provided that the distance between the  $B$  and  $D$  vertices  $d_T^{BD}$  was less than  $3 \cdot \sigma(d_T^{BD})$ .

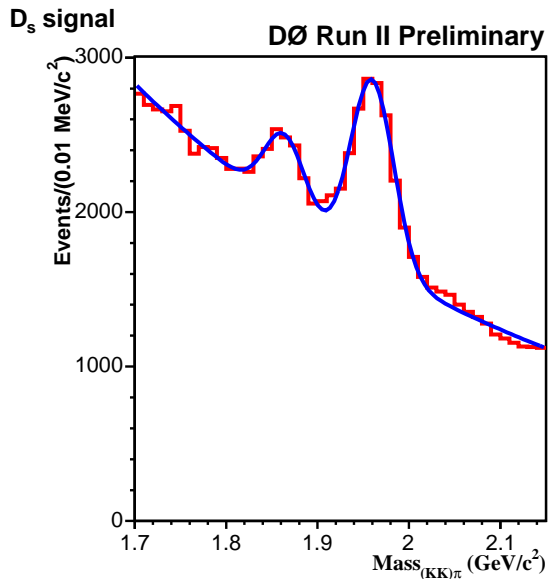


FIG. 1: All  $B_s$  candidates for the untagged sample for  $-0.01 < VPDL < 0.06$  cm.

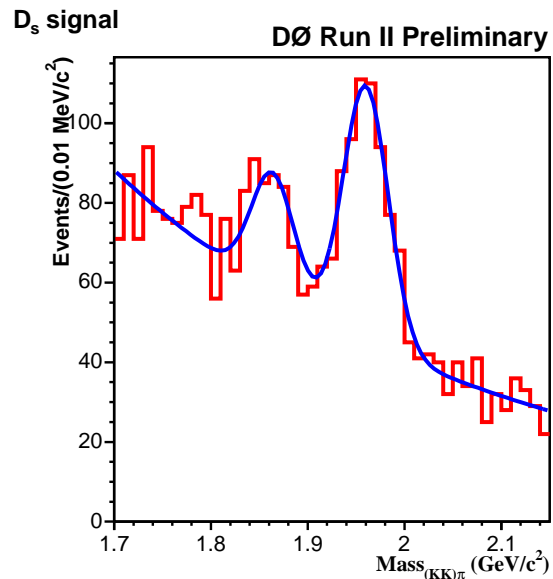


FIG. 2: All  $B_s$  candidates for the tagged sample for  $-0.01 < VPDL < 0.06$  cm.

The measured *visible proper decay length* (VPDL or  $x^M$ ) is defined as:

$$x^M = (\mathbf{d}_T^B \cdot \mathbf{P}_{xy}^{\mu D_s^-}) / (P_T^{\mu D_s^-})^2 \cdot M_B \quad (1)$$

The total number of  $D_s^-$  candidates in the mass peak is  $13339 \pm 277$ , while the number of  $D^\pm$  candidates is  $5019 \pm 292$ . For the  $B_s^0$  mixing measurement we use only  $B_s^0$  candidates with small visible proper decay lengths (see Figures 1 and 2). The number of  $B_s^0$  candidates with VPDL in range from  $-0.01$  cm to  $0.06$  cm is  $7037 \pm 208$  and  $376 \pm 31$  of them have an identified initial state flavor from the opposite-side  $\mu$  tag.

#### IV. INITIAL STATE TAGGING

The opposite-side tagging (OST) of the initial flavor of the  $B$  meson exploits the fact that in the  $b\bar{b}$  pair production there are always two particles in the final state containing b-quarks. Typically those are two jet events with two  $B$  mesons in two back-to-back jets, but the final state could also contain a  $B$  baryon and/or have more than two jets. In addition if the two b-jets originated from the flavor excitation or gluon splitting processes, the angle between the jets is not necessarily close to 180 degrees but varies over a wide range.

Purity, dilution and efficiency of the tagging are three useful parameters to describe the tagging performance. The purity of the tagging method was defined as  $\eta = N_{\text{correctly tagged events}} / N_{\text{total tagged events}}$ . The dilution is related to the purity with the simple formula  $\mathcal{D} = 2\eta - 1$ . Finally the tagging efficiency is defined as  $\epsilon = N_{\text{total tagged events}} / N_{\text{total events}}$ .

##### A. Tagging procedure

A combination of information from identified muons and reconstructed secondary vertices is used to construct the flavor tagging of  $B_s$ .

The tagging of the initial flavor of the  $B$  hadron is done with the likelihood ratio method. It is assumed that different discriminating variables  $x_1, \dots, x_n$  are constructed for a given event. For an initial  $b$ -quark flavor, the probability density function for a given variable  $x_i$  is denoted as  $f_i^b(x_i)$ , while for an initial anti- $b$  quark it is denoted as  $f_i^{\bar{b}}(x_i)$ . The combined tagging variable  $y$  is defined as:

$$y = \prod_{i=1}^n y_i; \quad y_i = \frac{f_i^{\bar{b}}(x_i)}{f_i^b(x_i)}. \quad (2)$$

If for given event the value of  $x_i$  is not defined,  $y_i$  is set to 1. The initial flavor is tagged as a  $b$  quark if  $y < 1$  and as an anti- $b$  quark if  $y > 1$ .

In practice, it is more convenient to define the tagging variable as:  $d = (1 - y)/(1 + y)$ . The  $d$  changes between -1 and 1.  $d > 0$  tags the initial  $B$  flavor as a  $b$  quark and  $d < 0$  tags the initial flavor as an anti- $b$  quark. For uncorrelated variables  $x_1, \dots, x_n$ ,  $d$  gives the best possible tagging performance and its absolute value gives a dilution of given event.

In this analysis, all discriminating variables were built for events with an additional muon opposite ( $\cos \phi(\mathbf{p}_\mu, \mathbf{p}_B) < 0.8$ ) the reconstructed  $B$  hadron.

If there are several muons satisfying this condition, then the muon with the largest number of hit layers in the muon system is chosen. If the muons have the same number of the hit layers, then maximal  $P_T$  is the next measure. For each such muon, the following discriminating variables were defined:

- charge of jet containing the muon:  $Q_J = \sum_i q^i p_T^i / \sum_i p_T^i$ , where the sum is taken over all charged particles, including the muon, with  $\Delta R = \sqrt{(\Delta\phi)^2 + (\Delta\eta)^2}$  with respect to the muon satisfying the condition  $\Delta R < 0.5$ .
- transverse momentum of the muon relative to the nearest jet multiplied by its charge,  $p_T^{rel} \cdot q_\mu$ .

In addition, a secondary vertex corresponding to the decay of a  $B$  hadron was searched for using all charged particles in the event. The muon was not required explicitly to be included in the secondary vertex. The secondary vertex should contain at least 2 particles with axial impact parameter significance greater than 3. The distance  $l_{xy}$  from the primary to the secondary vertex should satisfy the condition:  $l_{xy} > 4\sigma(l_{xy})$ . The details of the secondary vertex search can be found in [4].

The momentum of the secondary vertex  $\mathbf{p}_{SV}$  was defined as the sum of all momenta of particles included in the secondary vertex. A secondary vertex with  $\cos \phi(\mathbf{p}_{SV}, \mathbf{p}_B) < 0.8$  was included in the flavor tagging, and the secondary vertex charge  $Q_{SV}$  was defined as the third discriminating variable:  $Q_{SV} = \sum_i (q^i p_T^i)^{0.6} / \sum_i (p_T^i)^{0.6}$  where the sum was taken over all particles included in the secondary vertex. Particles from  $B \rightarrow \mu D_s X$  decay were explicitly excluded from the sum.

The probability density functions for all discriminating variables were constructed using a  $B \rightarrow \mu^+ \nu D^{*-}$  data sample with small decay lengths. In this sample, the non-oscillating decays  $B^0 \rightarrow \mu^+ \nu D^{*-}$  dominate. The ratios  $f_i^b(x_i)/f_i^{\bar{b}}(x_i)$  were computed separately for medium and tight-quality muons.

The analysis assumes that the tagging purity is the same for all  $B$  mesons because the opposite-side tagging information has little correlation with the reconstructed  $B$  meson candidate. This means that the results for the opposite-side tagger determined from  $B_d$  and  $B_u$  decays can be directly applied to the  $B_s$ . This assumption has been checked comparing dilutions obtained for semileptonic  $B_d$  and  $B_u$  samples as described in the next section.

## B. Dilutions for $B_d$ and $B_u$

$B_d$  and  $B_u$  mesons were selected using their semileptonic decays  $B \rightarrow \mu^+ \nu \bar{D}^0 X$  and were classified into two exclusive groups: “ $D^*$ ” sample, containing all events with reconstructed  $D^{*-} \rightarrow \bar{D}^0 \pi^-$  decays, and “ $D^0$ ” sample, containing all remaining events. Exploiting that semileptonic  $B$  decays are saturated by decays to  $D$ ,  $D^*$  and  $D^{**}$ , and the isotopic invariance, it was determined from simulation and available experimental results that the  $B_d^0$  (85%) and  $B^+$  (15%) decays give the main contributions to the “ $D^*$ ” sample. The  $D^0$  sample correspondingly has a 85% contribution from  $B^+$  and 15% contribution from  $B_d^0$  which causes the tiny oscillation in Figure 3.

We have repeated the  $\Delta m_d$  measurement described in DØ note 4330 [5] with increased statistics of the samples and a cut on transverse momentum of the  $D$  meson  $P_T^D > 5$  GeV to be consistent with the  $P_T$  spectrum of  $D_s^-$  meson. Figures 3, 4 show the results of this measurement. The VPDL bins from  $-0.01$  cm to  $0.05$  cm have the same bin width as was used for the  $B_s$  mixing measurement.

The  $B_d$  meson oscillation frequency was measured with the Opposite-Side Tagging algorithm to be equal to:

$$\begin{aligned} \Delta m_d &= 0.558 \pm 0.048 \text{ (stat.) } ps^{-1} \\ \eta_d &= 0.724 \pm 0.021 \text{ (stat.)} \\ \eta_u &= 0.734 \pm 0.015 \text{ (stat.)} \end{aligned} \tag{3}$$

This result is in good agreement with the world average of  $\Delta m_d = 0.502 \pm 0.007$  ps $^{-1}$ .

One of the purposes of this measurement is to extract the dilutions for reconstructed  $B_d$  and  $B_u$  mesons. The purities  $\eta_d$  and  $\eta_u$  are consistent within the statistical error. As an input to the  $B_s$  mixing measurement procedure we used purity value  $\eta_u = 0.734$  since the tagging algorithm was optimized using  $B_d$  sample.

The hypothesis that the dilution is independent on the  $B$  meson type has also been checked in Monte Carlo (MC).

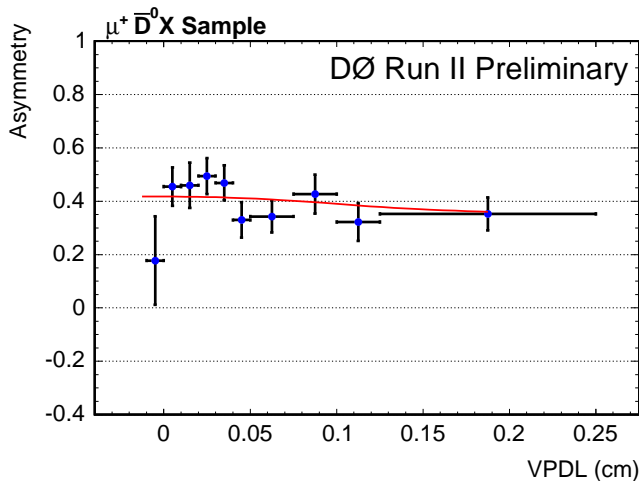


FIG. 3: The asymmetries in the  $\mu^+ D^0$  sample as a function of the visible proper decay length.

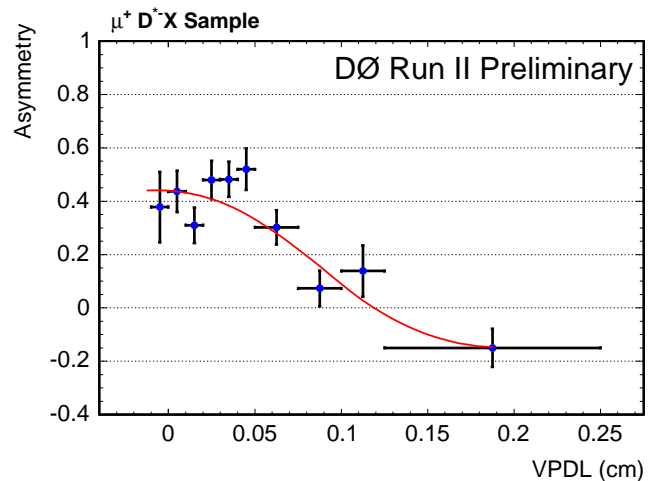


FIG. 4: The asymmetries in the  $\mu^+ D^*$  sample as a function of the visible proper decay length.

## V. TAGGED $B_s$ SAMPLE

Figure 1 shows all  $B_s$  candidates for the untagged sample for  $-0.01 < VPDL < 0.06$  cm.

### A. Mass Fitting Procedure

The number of  $B_s$  candidates in the untagged sample is quite large and allows us to fit a large statistics sample. However, once the data is flavor tagged into mixed and untagged samples and the data separated into bins of VPDL the statistics in each bin are very much reduced. To improve on the fitting, we first fit the full untagged sample ( $-0.01 < VPDL < 0.06$  cm) and then fix the mass and width of the  $D_s$  from that sample when the flavor tagged samples are fit. For fitting the untagged sample, single Gaussians are used to describe the  $D_s^\pm \rightarrow \phi\pi$  and  $D_s^\pm \rightarrow \phi\pi$  decays, and the background is modeled by an exponential.

## VI. EXPERIMENTAL OBSERVABLES $A_i$

Events were divided into 7 groups according to the measured VPDL. Intervals of VPDL for those groups are defined in Table I. The number of  $\mu^+ D_s^-$  events with positive and negative tags,  $N_i^{osc}$  and  $N_i^{non-osc}$ , in each interval  $i$  were determined from a fit of the  $D_s^-$  peak in the mass  $M(D_s^-)$  distribution.

The number of “non-oscillated” and “oscillated” events in each VPDL bin is given in Table I together with the corresponding errors derived from the fit.

bin	VPDL range, cm	$N_i^{non-osc}$	$\sigma(N_i^{non-osc})$	$N_i^{osc}$	$\sigma(N_i^{osc})$	$A_i$	$\sigma(A_i)$
1	-0.01 - 0	12.17	5.24	11.19	5.35	0.042	0.321
2	0 - 0.01	23.39	7.30	26.21	6.86	-0.057	0.203
3	0.01 - 0.02	24.79	8.62	34.28	8.25	-0.161	0.206
4	0.02 - 0.03	43.83	8.24	30.87	7.88	0.174	0.154
5	0.03 - 0.04	23.09	7.50	20.29	8.87	0.065	0.271
6	0.04 - 0.05	37.49	8.89	26.85	7.69	0.165	0.181
7	0.05 - 0.06	23.81	8.19	19.85	7.16	0.091	0.247

TABLE I:  $\mu^+ D_s^-$  sample. Definition of 7 intervals in VPDL. For each interval this table lists the measured number of  $D_s^-$  for the opposite sign and same sign as the tag  $N_i^{non-osc}, N_i^{osc}$ , and their statistical errors  $\sigma(N_i^{non-osc}), \sigma(N_i^{osc})$ , all determined from the fits of corresponding mass  $M_{D_s^-}$  distributions. Also listed are the measured asymmetries  $A_i$  and their errors  $\sigma(A_i)$ .

The experimental observables, asymmetry  $A_i$  in each VPDL bin, for this measurement were defined as:

$$A_i = \frac{N_i^{non-osc} - N_i^{osc}}{N_i^{non-osc} + N_i^{osc}}; \quad (4)$$

where  $N_i^{non-osc}$  is the number of events tagged as “non-oscillated” and  $N_i^{osc}$  is the number of events tagged as “oscillated”. Figure 5 shows the asymmetry defined above as a function of the visible proper decay length.

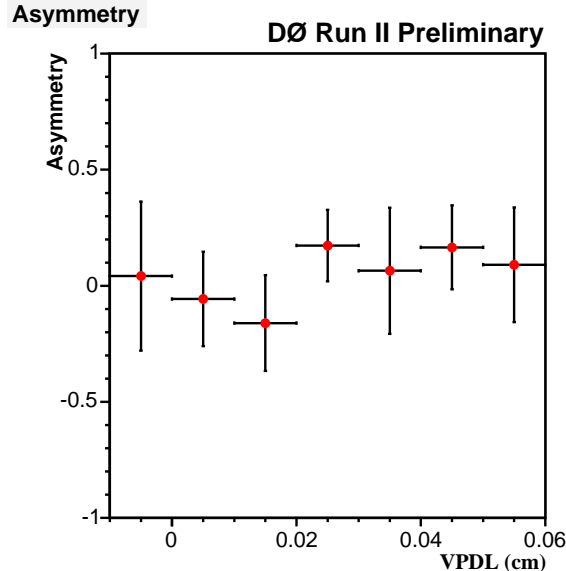


FIG. 5: The asymmetry in the  $D_s$  sample as a function of the visible proper decay length (VPDL).

## VII. FITTING PROCEDURE

The  $D_s^-$  sample is composed mostly of  $B_s^0$  mesons with some contributions from  $B_u$  and  $B_d$  mesons. The small contributions from b-baryons are neglected. The different species of  $B$  mesons behave differently with respect to oscillations. Neutral  $B_d^0$  and  $B_s$  mesons oscillate while charged  $B_u$  mesons do not, so we must take into account the different frequencies of oscillations during the fitting procedure.

For a given type of  $B$ -hadron (i.e.  $d$ ,  $u$ ,  $s$ ), the distribution of the visible proper decay length,  $x$ , is given by:

$$n_s^{non-osc/osc}(x) = \frac{K}{c\tau_{B_s}} \exp\left(-\frac{Kx}{c\tau_{B_s}}\right) \cdot 0.5 \cdot (1 \pm (2\eta - 1) \cos(\Delta m_s \cdot Kx/c)) \quad (5)$$

$$n_{D_s D_s}^{non-osc}(x) = n_{D_s D_s}^{osc}(x) = \frac{K}{c\tau_{B_s}} \exp\left(-\frac{Kx}{c\tau_{B_s}}\right) \cdot 0.5 \quad (6)$$

$$n_u^{non-osc}(x) = \frac{K}{c\tau_{B_u}} \exp\left(-\frac{Kx}{c\tau_{B_u}}\right) \cdot (1 - \eta) \quad (7)$$

$$n_u^{osc}(x) = \frac{K}{c\tau_{B_u}} \exp\left(-\frac{Kx}{c\tau_{B_u}}\right) \cdot \eta$$

$$n_d^{non-osc/osc}(x) = \frac{K}{c\tau_{B_d}} \exp\left(-\frac{Kx}{c\tau_{B_d}}\right) \cdot 0.5 \cdot (1 \mp (2\eta - 1) \cos(\Delta m_d \cdot Kx/c)) \quad (8)$$

where  $K = P_T^{\mu D_s^-} / P_T^B$  is a K-factor reflecting the difference between the observable and true momentum of the  $B$ -hadron (for more on the K-factor see Section VIII), and  $\tau$  is the lifetime of  $B$ -hadrons taken from the PDG [7]. The  $D_s^\pm$  charge has different correlations with the  $b$ -quark flavor in the  $B_u$  or  $B_d$  decays with respect to the  $B_s$  semileptonic decays. The equations 7 and 8 take this into account.

The transition to the measured VPDL,  $x^M$ , is achieved by the integration over the  $K$ -factors and resolution functions:

$$N_{(d,u,s),j}^{osc, non-osc}(x^M) = \int dx Res_j(x - x^M, x) \cdot Eff_j(x) \int dK D_j(K) \cdot \theta(x) \cdot n_{(d,u,s),j}^{osc, non-osc}(x, K). \quad (9)$$

$Res_j(x - x^M, x)$  is the detector resolution of the VPDL and  $Eff_j(x)$  is the reconstruction efficiency for a given decay channel  $j$  of this type of  $B$  meson. Both are determined from the MC simulation.

The expected number of oscillated/non-oscillated events in the  $i$ -th bin of VPDL is equal to

$$N_i^{e,osc/non-osc} = \int_i dx^M \left( \sum_{f=u,d,s} \sum_j (Br_j \cdot N_{f,j}^{osc/non-osc}(x^M)) \right) \quad (10)$$

The integration  $\int_i dx^M$  is taken over a given interval  $i$ , the sum  $\sum_j$  is taken over all decay channels  $B \rightarrow \mu^+ \nu D^{*-} X$  and  $Br_j$  is the branching ratio of a given channel  $j$ . The latest PDG values [7] were used for the  $B$  decay branching fractions.

Finally, the expected value  $A_i^e$  for interval  $i$  of the measured VPDL is given by formula (4) with  $N_i^{non-osc}$  and  $N_i^{osc}$  substituted by  $N_i^{e,non-osc}$  and  $N_i^{e,osc}$ .

In order to set a limit on the value of  $\Delta m_s$ , we chose to use a technique called the amplitude fit method [8]. This technique requires us to modify equation (5) to the following form

$$n_s^{non-osc/osc}(x) = \frac{K}{c\tau_{B_s}} \exp\left(-\frac{Kx}{c\tau_{B_s}}\right) \cdot 0.5 \cdot (1 \pm (2\eta - 1) \cos(\Delta m_s \cdot Kx/c)) \cdot \mathcal{A} \quad (11)$$

where  $\mathcal{A}$  is now the only fit parameter.

The fitted values of  $\mathcal{A}$  as a function of  $\Delta m_s$  were determined from the minimization of a  $\chi^2(\mathcal{A})$  defined as:

$$\chi^2(\mathcal{A}) = \sum_i \frac{(A_i - A_i^e(\mathcal{A}))^2}{\sigma^2(A_i)} \quad (12)$$

The values of  $\Delta m_s$  were changed from  $1 \text{ ps}^{-1}$  to  $10 \text{ ps}^{-1}$  with a step size of  $1 \text{ ps}^{-1}$ . For each value of  $\Delta m_s$  the fitted value of  $\mathcal{A}$  and its error were determined.

### VIII. INPUTS TO $A_i^e$

We have used the measured parameters for  $B$  mesons from the PDG [7] as inputs for the fitting procedure:  $c\tau_{B^+} = 501 \mu\text{m}$ ,  $c\tau_{B^0} = 460 \mu\text{m}$ ,  $c\tau_{B_s} = 438 \mu\text{m}$ , and  $\Delta m_d = 0.502 \text{ ps}^{-1}$ .

The latest PDG values were also used to determine the branching fractions of decays contributing to the  $D_s^-$  sample. We use the event generator EvtGen [9] since this code was developed specifically for the simulation of  $B$  decays. For those branching fractions not given in the PDG, we used the values provided by EvtGen. Taking into account the corresponding branching rates and reconstruction efficiencies, we determined the following contributions to our signal region from the various processes:

- $B_s^0 \rightarrow \mu^+ \nu D_s^-$  : 20.6%;
- $B_s^0 \rightarrow \mu^+ \nu D_s^{*-} \rightarrow \mu^+ \nu D_s^-$  : 57.2%;
- $B_s^0 \rightarrow \mu^+ \nu D_{s0}^{*-} \rightarrow \mu^+ \nu D_s^-$  : 1.4%;
- $B_s^0 \rightarrow \mu^+ \nu D_{s1}^{\prime-} \rightarrow \mu^+ \nu D_s^-$  : 2.9%;
- $B_s^0 \rightarrow D_s^+ D_s^- X$ ;  $D_s^- \rightarrow \mu \nu X$  : 11.3%;
- $B^+ \rightarrow DD_s^- X$ ;  $D \rightarrow \mu \nu X$  : 3.2%;
- $B^0 \rightarrow DD_s^- X$ ;  $D \rightarrow \mu \nu X$  : 3.4%;

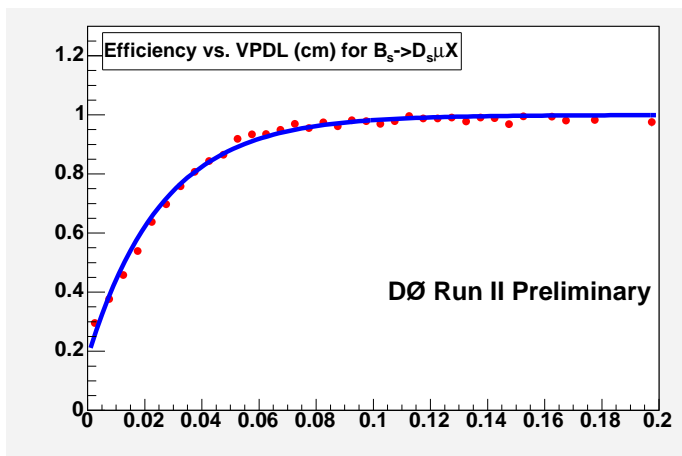


FIG. 6: Efficiency as function of VPDL(cm) for  $B_s \rightarrow \mu^+ \nu D_s^- X$ .

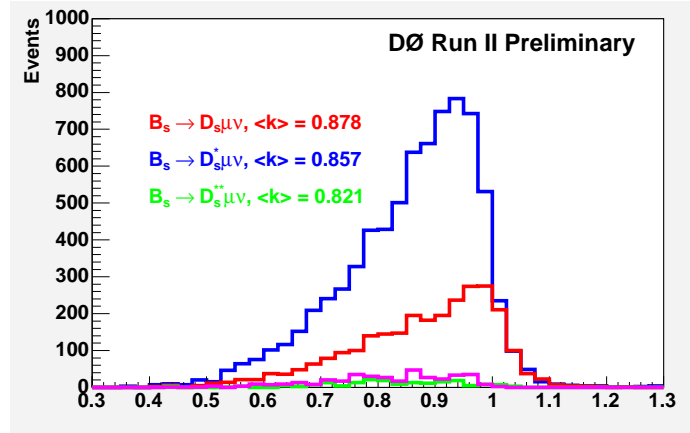


FIG. 7: K-factors for  $B_s^0 \rightarrow \mu^+ \nu D_s^-$ ;  $B_s^0 \rightarrow \mu^+ \nu D_s^{*-}$   $\rightarrow \mu^+ \nu D_s^-$ ;  $B_s^0 \rightarrow \mu^+ \nu D_{s0}^{*-} \rightarrow \mu^+ \nu D_s^-$ ;  $B_s^0 \rightarrow \mu^+ \nu D_{s1}^{\prime-} \rightarrow \mu^+ \nu D_s^-$  processes.

In the above numbers, the reconstruction efficiency does not include any lifetime cuts. We determined the efficiency of the lifetime selections for the sample as a function of VPDL as shown in Figure 6 for the decay  $B_s \rightarrow \mu^+ \nu D_s^- X$ .

The background due to  $c\bar{c}$  pairs originating from gluon splitting is an important contributor to the sample composition since they can produce the  $\mu D_s$  signature. For this to happen one c-quark must fragment to a  $D_s$  meson and the other c-quark must decay semileptonically. The OST used for this analysis requires a muon on the opposite side and therefore should suppress much of the  $c\bar{c}$  contribution.

We estimate the  $c\bar{c}$  contribution to the  $\mu D_s$  sample by using our estimate of this contribution to the  $\mu D^0$  sample used for the lifetime ratio analysis [6]. The  $c\bar{c}$  contribution was determined to be  $3.5 \pm 2.5\%$  after flavor tagging. The VPDL distribution for  $c\bar{c}$  events was determined from MC.

Semileptonic  $B$  decays necessarily have a neutrino present in the decay chain making a precise determination of the kinematics for the  $B$  meson impossible. In addition other neutrals or non-reconstructed charged particles can be present in the decay chain of the  $B$  meson. This leads to a bias towards smaller values of the  $B$  momentum calculated using the reconstructed particles. A common practice to correct this bias is to scale the measured momentum of the  $B$  by a  $K$ -factor, which takes into account the effects of neutrinos and other lost (or not used) particles. The  $K$ -factor was estimated from the MC simulation. For this analysis it was defined as:

$$K = p_T(\mu D_s^-) / p_T(B), \quad (13)$$

where  $p_T$  denotes the absolute value of transverse momentum.

In determining the  $K$ -factor, generator level information was used for the computation of  $p_T$ . Following the definition used in (13), the  $K$ -factors for all considered decays were calculated. Figure 7 shows the distributions of the  $K$ -factors for the semileptonic decays of the  $B_s$ . As expected, the  $K$ -factors for  $D_s^{*-}$ ,  $D_{s0}^{*-}$  and  $D_{s1}^{\prime-}$  have lower mean values because more decay products are lost. Note that since the  $K$ -factors in (13) were defined as the ratio of transverse momenta, they can exceed unity.

### A. VPDL resolution

The decay length resolution for all samples was taken from the MC simulation and was parameterized by the sum of three Gaussians in the case of semileptonic  $B_s^0$  decays and by two Gaussians in all other cases.

### B. Tuning procedure for VPDL resolution

One of the most important issues for  $B_s$  mixing is the proper time resolution. We use MC simulation to determine the resolution, however this assumes the uncertainties on the tracks are properly modeled in MC. A procedure for reconstruction and propagation of the tracks assigns an error matrix to each track. An element in this matrix which corresponds to the impact parameter (IP) error is the most important one for the secondary vertex reconstruction.

A technique to determine the IP errors with better accuracy was developed at DELPHI [10]. The IP error,  $\sigma_{IP}$ , depends on the number of the SMT hits on the track, geometrical location of the hit silicon sensors, the cluster width of the SMT hits, and the track momentum  $p$  and polar angle  $\theta$ . We used the following functional form to fit this dependence:

$$\begin{aligned} \ln(\sigma_{IP}^2)|_{V(p,\theta)>c} &= a + b \cdot (V(p,\theta) - c)^2, \\ \ln(\sigma_{IP}^2)|_{V(p,\theta)<c} &= a \end{aligned} \quad (14)$$

where  $V(p,\theta) = -\ln(p^2 \sin^3 \theta)$ . The parameters  $a$ ,  $b$  and  $c$  depend on the number of SMT hits, and their configuration and cluster width.

The  $\sigma_{IP}^2$  assigned by the tracking can be compared with the “true” IP resolution determined from the impact parameter distributions for the tracks coming from the primary vertex. We selected such tracks in events which passed QCD triggers, and removed tracks from long lived particles such as  $K_s$  and  $\Lambda$ . The same tuning procedure was applied to the MC tracks. Finally, we have four sets of the parameters  $a$ ,  $b$  and  $c$  for each hit configuration:

- Assigned track errors for data:  $a_{track}^{data}, b_{track}^{data}, c^{data}$
- “True” track errors for data:  $a_{true}^{data}, b_{true}^{data}, c^{data}$
- Assigned track errors for MC:  $a_{track}^{mc}, b_{track}^{mc}, c^{mc}$
- “True” track errors for MC:  $a_{true}^{mc}, b_{true}^{mc}, c^{mc}$

The parameter  $c$  was determined from the assigned track errors and fixed to this value when we fit the “true” track errors. We use these sets to scale the track errors for data and MC. In addition the MC tracks were smeared to have the same “true” errors as the data ones. The dependence of the scale factors on hit configurations, track momentum and polar angle is taken into account.

Signal MC was used to determine how the tuning procedure changes the VPDL resolution function. The fractions and widths of the gaussians have been fixed to the values before tuning. The overall scale factor on the VPDL resolution was found to be equal to  $SF = 1.095$ . Figure 8 shows the VPDL resolution before and after the tuning procedure. The fit shows good agreement with the assumption that the scale factor is the same for all components.

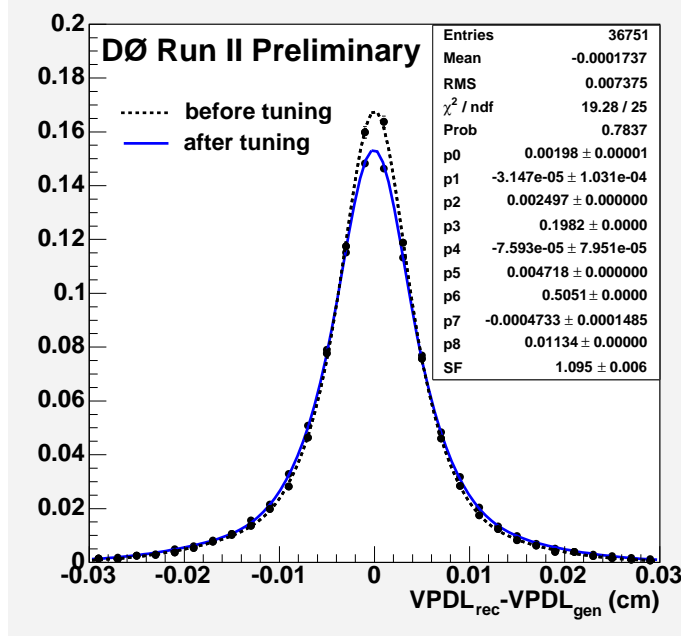


FIG. 8: Distribution of (reconstructed VPDL - generated VPDL) for decay  $B_s \rightarrow \mu^+ \nu D_s^- X$  before and after the tuning procedure.

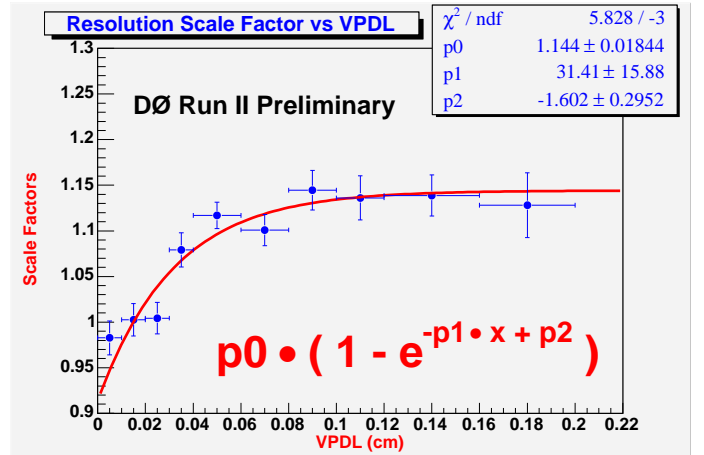


FIG. 9: The scale factor in the VPDL resolution increases as a function of VPDL.

The VPDL resolutions have been found to depend on the VPDL. We describe this effect by using a variable scale factor  $SF$  for the VPDL resolution (Fig. 9). This dependence was implemented in the asymmetry fitting procedure.

## IX. RESULTS

Figure 10 shows the dependence of the parameter  $\mathcal{A}$  and its error on  $\Delta m_s$ . A 95% confidence level limit on the oscillation frequency  $\Delta m_s > 5.2 \text{ ps}^{-1}$  and a sensitivity  $5.1 \text{ ps}^{-1}$  were obtained with statistical error only.

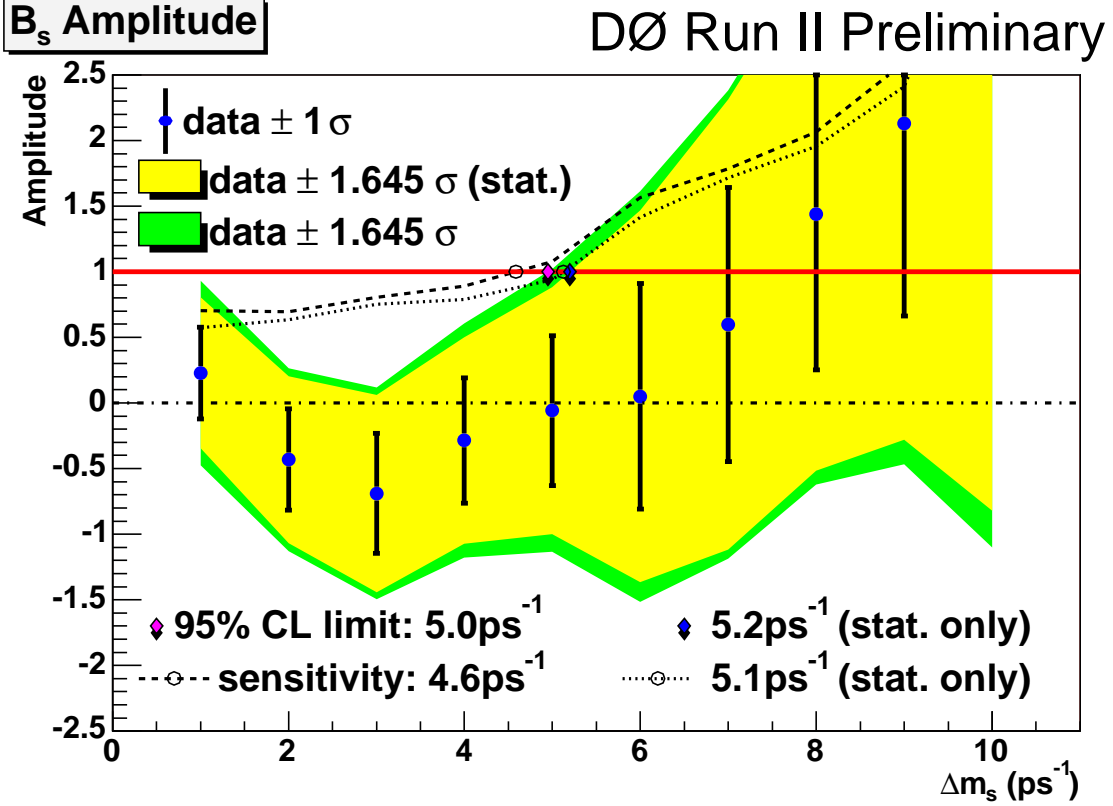


FIG. 10:  $B_s^0$  oscillation amplitude with statistical and systematic errors.

## X. SYSTEMATIC UNCERTAINTIES AND CROSS CHECKS

All studied contributions to the systematic uncertainty of the amplitude are listed in Table II. The resulting systematic errors were obtained using the following formula [8]:

$$\sigma_{\mathcal{A}}^{sys} = \Delta \mathcal{A} + (1 - \mathcal{A}) \frac{\Delta \sigma_{\mathcal{A}}}{\sigma_{\mathcal{A}}} \quad (15)$$

and summed in quadrature. The result is shown in Figure 10.

## XI. CONCLUSIONS

Using a signal of 13.3k  $B_s^0 \rightarrow \mu^+ \nu D_s^- X$  decays where  $D_s \rightarrow \phi \pi$ ,  $\phi \rightarrow KK$  and an opposite-side flavor tagging algorithm, we performed a search for  $B_s^0 - \bar{B}_s^0$  oscillations. We obtain a 95% confidence level limit on the oscillation frequency  $\Delta m_s > 5.0 \text{ ps}^{-1}$  and a sensitivity  $4.6 \text{ ps}^{-1}$ .

## Acknowledgments

We thank the staffs at Fermilab and collaborating institutions, and acknowledge support from the Department of Energy and National Science Foundation (USA), Commissariat à l'Énergie Atomique and CNRS/Institut National

TABLE II: Systematic uncertainties on the amplitude. The shifts of both the measured amplitude,  $\Delta\mathcal{A}$ , and its statistical uncertainty,  $\Delta\sigma$ , are listed

Osc. frequency		1 ps <sup>-1</sup>	2 ps <sup>-1</sup>	3 ps <sup>-1</sup>	4 ps <sup>-1</sup>	5 ps <sup>-1</sup>	6 ps <sup>-1</sup>	7 ps <sup>-1</sup>	8 ps <sup>-1</sup>	9 ps <sup>-1</sup>	10 ps <sup>-1</sup>
Amplitude	$\mathcal{A}$	0.228	-0.432	-0.690	-0.286	-0.057	0.051	0.598	1.441	2.130	3.234
Stat. uncertainty	$\sigma_{stat}$	0.349	0.386	0.457	0.479	0.572	0.860	1.043	1.189	1.466	2.465
$\eta_s = 0.719$	$\Delta\mathcal{A}$	+0.010	-0.028	-0.043	-0.018	-0.003	+0.008	+0.044	+0.097	+0.142	+0.217
	$\Delta\sigma$	+0.024	+0.026	+0.031	+0.033	+0.039	+0.059	+0.071	+0.081	+0.113	+0.169
$c\bar{c}$ : 6%	$\Delta\mathcal{A}$	+0.044	-0.042	-0.058	-0.012	+0.004	-0.018	+0.013	+0.114	+0.175	+0.471
	$\Delta\sigma$	+0.034	+0.022	+0.026	+0.027	+0.033	+0.068	+0.086	+0.097	+0.124	+0.270
$D_s D_s$ : 21.6%	$\Delta\mathcal{A}$	+0.014	-0.045	-0.070	-0.032	-0.007	+0.015	+0.077	+0.156	+0.227	+0.342
	$\Delta\sigma$	+0.038	+0.044	+0.052	+0.054	+0.064	+0.095	+0.116	+0.130	+0.174	+0.269
$c\tau_{B_s} = 455\mu m$	$\Delta\mathcal{A}$	+0.004	-0.004	-0.005	+0.001	+0.001	+0.000	+0.005	+0.014	+0.018	+0.040
	$\Delta\sigma$	+0.003	+0.002	+0.003	+0.002	+0.003	+0.007	+0.006	+0.008	+0.023	+0.034
same eff. dependence for signal and bkg	$\Delta\mathcal{A}$	+0.011	-0.004	-0.011	-0.005	-0.003	-0.006	+0.000	+0.018	+0.028	+0.041
	$\Delta\sigma$	+0.004	+0.004	+0.005	+0.005	+0.006	+0.009	+0.011	+0.013	+0.028	+0.028
Resolution $S.F. = 2$ for background	$\Delta\mathcal{A}$	-0.005	+0.002	+0.007	+0.004	+0.003	+0.006	+0.003	-0.009	-0.015	-0.003
	$\Delta\sigma$	-0.002	-0.002	-0.003	-0.003	-0.004	-0.006	-0.125	-0.010	+0.000	-0.011
$D_s$ mass changed to 1.9601 + 0.0007	$\Delta\mathcal{A}$	-0.003	-0.004	+0.020	-0.003	+0.016	+0.023	-0.024	-0.016	-0.054	-0.124
	$\Delta\sigma$	+0.006	+0.000	-0.005	+0.013	+0.017	-0.006	+0.000	+0.034	+0.053	+0.053
$D_s$ sigma changed to 0.02336 - 0.00076	$\Delta\mathcal{A}$	-0.041	-0.034	-0.006	+0.010	+0.136	+0.186	-0.075	-0.114	+0.002	-0.009
	$\Delta\sigma$	+0.014	+0.015	+0.010	+0.048	+0.025	+0.031	-0.002	+0.057	+0.101	+0.119
$D^+$ mass changed to 1.8641 - 0.0016	$\Delta\mathcal{A}$	-0.040	-0.006	+0.023	+0.040	+0.062	+0.065	-0.015	-0.046	-0.063	-0.162
	$\Delta\sigma$	+0.006	+0.001	+0.007	+0.019	+0.021	+0.002	+0.002	+0.035	+0.067	+0.071
Bkg. from wrong sign combination	$\Delta\mathcal{A}$	-0.103	+0.008	+0.035	-0.020	-0.002	+0.066	-0.016	-0.227	-0.412	-0.756
	$\Delta\sigma$	-0.006	+0.002	+0.004	+0.016	+0.019	+0.003	+0.003	+0.022	+0.042	-0.041
Bkg. parametrized by straight line	$\Delta\mathcal{A}$	-0.028	+0.002	-0.044	-0.124	+0.033	+0.146	-0.080	-0.095	-0.014	-0.084
	$\Delta\sigma$	+0.042	+0.023	+0.024	+0.070	+0.070	+0.115	+0.126	+0.215	+0.251	+0.276
mass bin smaller by 50%	$\Delta\mathcal{A}$	-0.051	+0.023	+0.089	+0.002	-0.013	+0.151	+0.246	+0.021	-0.298	-0.471
	$\Delta\sigma$	-0.029	-0.010	-0.031	-0.030	-0.021	-0.120	-0.123	-0.116	-0.124	-0.194
$\Delta\Gamma/\Gamma = 0.2$	$\Delta\mathcal{A}$	-0.000	-0.001	-0.001	-0.001	-0.001	+0.001	+0.002	+0.002	+0.002	+0.002
	$\Delta\sigma$	+0.000	+0.001	+0.001	+0.001	+0.001	+0.001	+0.001	+0.001	+0.014	+0.002
Resolution $S.F. = 1.115$	$\Delta\mathcal{A}$	+0.006	-0.003	-0.021	-0.011	+0.002	+0.001	+0.038	+0.154	+0.247	+0.233
	$\Delta\sigma$	+0.001	+0.007	+0.013	+0.020	+0.030	+0.061	+0.100	+0.139	+0.198	+0.266
K-factor variation 2%	$\Delta\mathcal{A}$	+0.009	+0.012	-0.000	-0.035	-0.011	-0.027	-0.095	-0.134	-0.096	-0.264
	$\Delta\sigma$	-0.003	+0.003	-0.005	+0.002	-0.016	-0.037	-0.005	-0.028	-0.053	-0.290
Total	$\sigma_{tot}$	0.427	0.424	0.490	0.541	0.655	0.951	1.084	1.254	1.577	2.636

de Physique Nucléaire et de Physique des Particules (France), Ministry for Science and Technology and Ministry for Atomic Energy (Russia), CAPES, CNPq and FAPERJ (Brazil), Departments of Atomic Energy and Science and Education (India), Colciencias (Colombia), CONACyT (Mexico), Ministry of Education and KOSEF (Korea), CONICET and UBACyT (Argentina), The Foundation for Fundamental Research on Matter (The Netherlands), PPARC (United Kingdom), Ministry of Education (Czech Republic), Natural Sciences and Engineering Research Council and West-Grid Project (Canada), BMBF (Germany), A.P. Sloan Foundation, Civilian Research and Development Foundation, Research Corporation, Texas Advanced Research Program, and the Alexander von Humboldt Foundation.

- 
- [1] This limit is derived by combining limits from 13 different searches. Global fits to the CKM unitarity triangle are described in M. Battaglia *et al.*, “The CKM matrix and the unitarity triangle,” arXiv:hep-ph/0304132, Oct. 2003.
  - [2] S. Catani, Yu.L. Dokshitzer, M. Olsson, G. Turnock, B.R. Webber, Phys.Lett. **B269** (1991) 432.
  - [3] T. Sjöstrand *et. al.* hep-ph/0108264
  - [4] DELPHI Collab., *b-tagging in DELPHI at LEP*, Eur. Phys. J. **C32** (2004), 185-208
  - [5] G. Borisov, S. Burdin, A. Nomerotski, *B<sub>d</sub> flavor oscillations with opposite side muon tagging*
  - [6] G. Borisov, S. Burdin, A. Nomerotski, *Measurement of Lifetime Ratio for Neutral and Charged B Mesons*
  - [7] S. Eidelman *et al*, Phys. Lett. **B592**, 1 (2004)
  - [8] H.G. Moser, A. Roussarie Nucl.Instrum.Meth.A384:491-505,1997
  - [9] D.J. Lange, NIM A 462 (2001) 152; for details see <http://www.slac.stanford.edu/~lange/EvtGen>
  - [10] G. Borisov and C. Mariotti, NIM A 372 (1996) 181-187